Dossier

This paper is a part of the hereunder thematic dossier published in OGST Journal, Vol. 68, No. 1, pp. 3-178 and available online here

Cet article fait partie du dossier thématique ci-dessous publié dans la revue OGST, Vol. 68, n°1, pp. 3-178 et téléchargeable ici

DOSSIER Edited by/Sous la direction de : **A. Sciarretta, F. Badin et J. Bernard**

RHEVE 2011: International Conference on Hybrid and Electric Vehicles

RHEVE 2011 : Conférence internationale sur les véhicules hybrides et électriques

Oil & Gas Science and Technology – Rev. IFP Energies nouvelles, Vol. 68 (2013), No. 1, pp. 3-178

Oil & Gas Science and Technology – Rev. IFP Energies nouvelles, Vol. 68 (2013), No. 1, pp. 35-50

DOI: 10.2516/ogst/2012100

IFP Energies nouvelles International Conference
Rencontres Scientifiques d'IFP Energies nouvelles

RHEVE 2011: International conference on hybrid and electric vehicles
RHEVE 2011 : Conférence internationale sur les véhicules hybrides et électriques

Optimization of Hybrid Power Trains by Mechanistic System Simulations

T. Katrašnik[1]* and J.C. Wurzenberger[2]

[1] *University of Ljubljana, Faculty of Mechanical Engineering, Aškerčeva 6, 1000 Ljubljana - Slovenia*
[2]*AVL List GmbH, Hans List Platz 1, A-8020, Graz - Austria*
e-mail: tomaz.katrasnik@fs.uni-lj.si

* Corresponding author

Résumé — Optimisation de groupes motopropulseurs électriques hybrides par simulation du système mécanique — L'article présente un modèle de simulation au niveau mécanique destiné à la modélisation de topologies de véhicules hydrides et conventionnels. L'article décrit l'interaction dynamique entre différents domaines : moteur à combustion interne, dispositifs de post-traitement d'échappement, composants électriques, chaîne cinématique mécanique, circuit de refroidissement et les unités de contrôle correspondantes. Afin d'obtenir un rapport correct entre précision, prévisibilité et vitesse de calculs du modèle, un découplage innovant du domaine temporel est présenté, lequel est basé sur l'application à différents domaines, d'étapes d'intégration spécifiques au domaine et sur un couplage inter-domaines cohérent ultérieur des flux. En outre, une structure de calculs efficace permettant la simulation du transport d'espèces gazeuses actives et passives est introduite de manière à combiner l'efficacité des calculs à la nécessité d'une modélisation du transport des polluants dans le circuit des gaz. L'applicabilité et la versatilité du modèle de simulation au niveau mécanique sont présentées au moyen d'analyses des phénomènes transitoires provoqués par l'interdépendance élevée des sous-systèmes, c'est-à-dire les domaines. Les résultats obtenus pour les véhicules hybrides sont comparés à ceux obtenus pour les véhicules conventionnels afin de mettre l'accent sur les différences des régimes opératoires de composants particuliers inhérents à une topologie particulière du groupe motopropulseur.

Abstract* — *Optimization of Hybrid Power Trains by Mechanistic System Simulations — *The paper presents a mechanistic system level simulation model for modeling hybrid and conventional vehicle topologies. The paper addresses the dynamic interaction between different domains: internal combustion engine, exhaust after treatment devices, electric components, mechanical drive train, cooling circuit system and corresponding control units. To achieve a good ratio between accuracy, predictability and computational speed of the model an innovative time domain decoupling is presented, which is based on applying domain specific integration steps to different domains and subsequent consistent cross-domain coupling of the fluxes. In addition, a computationally efficient framework for transporting active and passive gaseous species is introduced to combine computational efficiency with the need for modeling pollutant transport in the gas path. The applicability and versatility of the mechanistic system level simulations model is presented through analyses of transient phenomena caused by the high interdependency of the sub-systems,* i.e. *domains. Results of a hybrid vehicle are compared to results of a conventional vehicle to highlight differences in operating regimes of particular components that are inherent to particular power train topology.*

INTRODUCTION

Global concerns on sustainable energy use and environmental protection call for innovative power train technologies. Among the alternative power trains being investigated, the Hybrid Electric Vehicle (HEV) consisting of an Internal Combustion Engine (ICE) and an Electric Machine (EM) are considered as a viable short to mid term solution due to the use of a smaller battery pack and due to their similarities with conventional vehicles. HEV incorporate multiple energy sources and multiple energy converters featuring many available patterns of combining the power flows to meet given load requirements. Additionally, due to the multiple power sources, there exist several power train topologies and a broad variety of different strategies to control the power sources, resulting in different vehicle performance and operation characteristics. Moreover, dynamic interactions among various components and their multidisciplinary nature additionally increase the complexity of the system analyses.

For such complex systems, the application of system simulations is indispensable during the early development phase. It allows a cost and time efficient identification of the most promising solutions and therefore it helps reducing the amount of expensive experimental validation on test benches. To efficiently support the development during early concept and design phases it is required that simulation models feature a high level of predictability and high computational speed. Especially the predictability strongly influences the potential of system simulations to support the development of power trains in very early development stages where measurements are not yet (fully) available. The application of predictive approaches also significantly reduces the time needed to set up the models, since potentially only a limited number of physically based parameters needs to be adjusted, which reduces the workload compared to the effort required to populate map based models and to train surrogate models. Moreover, physically based models also ensure adequacy of results when optimizing power trains, since a mechanistic modeling basis enables adequate response to changed parameters of individual components and adequate interaction between the components on the system level.

The addressed facts also clearly favor the application of mechanistic system level simulation models for simulating transient drive cycles. On the system level, there is a great challenge in establishing an appropriate balance between the level of detail of the model and its prediction accuracy [1]. This is particularly challenging for models of internal combustion engines [1]. Frequently, non-mechanistic engine model approaches like maps [2, 3] or surrogate models [4] are used to model the internal combustion engines. Such models might have significant limitations when applied to transient conditions that are far from steady-state [1, 5, 6]. However, also more sophisticated methodologies for estimating transient engine performance from steady-state maps [1], might not be sufficiently accurate, since during transient operation performance and particularly emissions of the engines significantly differ from the corresponding steady-state values as presented in [7-9]. This is even more pronounced for turbocharged engines with Exhaust Gas Recirculation (EGR). It is therefore advantageous to use mechanistic engine models, since they inherently consider changes in engine controls, thermal behavior of the engine, variations in gas state and composition as well as turbocharger lagging if turbocharger is included, which enable more adequate modeling of engine performance and production of emissions.

Recently, many commercial and non-commercial system level simulation models and modeling approaches for modeling hybrid and plug-in hybrid vehicles have been presented [5, 6, 10-13]. The models in the cited studies differ in the level of details of components models and also in the overall model structure, however a common approach of all cited studies is that they do not rely on mechanistic engine models. This influences their accuracy during the transient drive cycles and their predictability if modifying control strategies and particularly if scaling the components.

The presented system level model of the hybrid vehicle comprises different domains as shown in Figure 1: internal combustion engine, exhaust aftertreatment devices, electric components, mechanical drive train, cooling circuit system and corresponding control units. This requires a careful selection of the physical depth of the models used to describe phenomena in different domains with the aim to harmonize their accuracies, which enables optimizing the performance of the overall model. Moreover, the characteristic time scales of the addressed domains differ significantly, which typically results in a stiff system of equations [14]. Therefore the performance of the model is further enhanced by introducing tailored solver techniques suited to account for characteristic time scales of individual domains. These domains represent sub-matrices in the overall system matrix, which are integrated with time steps that correspond to characteristic time scales of the phenomena in the domains.

To expose the complex interaction between domains presented in Figure 1, the paper presents the analysis of the performance and emissions of a hybrid electric vehicle. Results of the hybrid electric vehicle are compared to the results of a conventional vehicle to

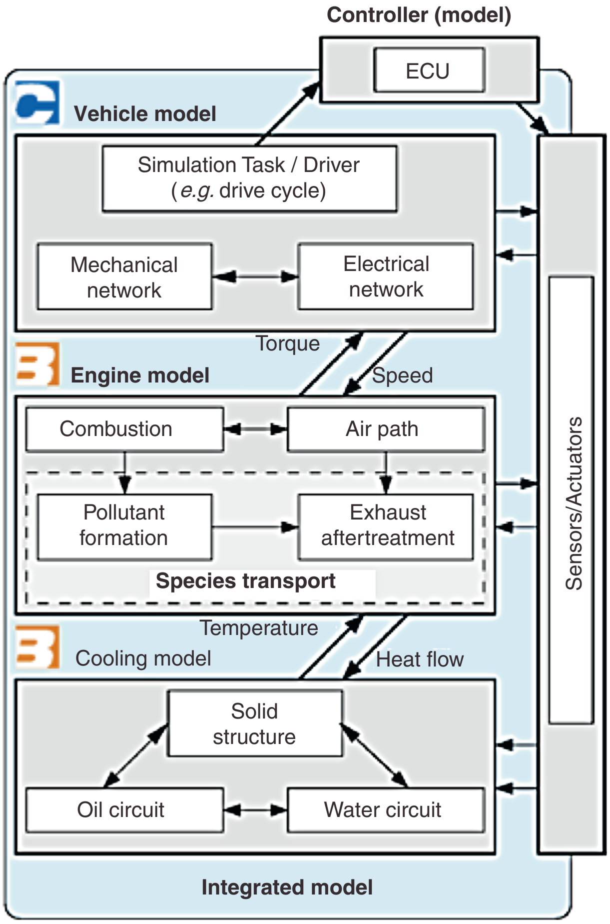

Figure 1

Interaction of integrated plant model with engine control.

highlight potential differences in operating regimes of particular components that are inherent to particular power train topology. Therefore, care is devoted to phenomena caused by the high interdependency of the domains, which also highlights the applicability and versatility of system level simulations featuring the mechanistic modeling depth. In this context, cross-influences between control strategies, electric components, EGR, turbocharging, heating up of the engine and catalyst light-off are investigated in the light of energy consumption and exhaust emissions.

As Diesel and lean-gasoline engines potentially have substantial fuel economy benefits over the conventional gasoline engines, there is a growing interest in the use of lean-burn engines in hybrid and plug-in hybrid vehicles [5, 6]. Due to this and due to the fact that Diesel engines need to be equipped with the sophisticated exhaust gas aftertreatment devices to be able to comply with the emission regulation, Diesel engine powered vehicles are analyzed in this study. Moreover, a turbocharged Diesel engine with EGR that is equipped with a Diesel Oxidation Catalyst (DOC), Diesel Particulate Filter (DPF) and Selective Catalytic Reduction converter (SCR) offers a good basis to present interdependency of the domains.

1 INTERACTION OF THE DOMAINS

To enhance the performance of the overall hybrid vehicle model it is necessary to analyze the characteristic time scales of different domains and the nature of their interaction. This forms the basis of the innovative time domain decoupling that allows for substantial reduction in the computational time of the overall model.

1.1 Mechanical System

The mechanical system of the vehicle (*Fig. 2*) is represented as the multibody system, which is mainly described through rotational degrees of freedom [15]. If explicit time schemes are used, which is the case in the presented analysis, time step lengths in the order of 1 ms are commonly used to integrated the mechanical system [15]. This is reasonable, since the typical response times of the mechanical system in vehicle driving dynamics are much larger compared to the stated integration time step. The mechanical system is represented by the following equation system (more details on the mechanical model are given in [15]):

$$\begin{pmatrix} \mathbf{M} & \mathbf{B} \\ \mathbf{C} & \mathbf{D} \end{pmatrix} \cdot \begin{pmatrix} \mathbf{a} \\ \mathbf{m} \end{pmatrix} = \begin{pmatrix} 0 \\ \mathbf{F} \end{pmatrix} \tag{1}$$

where **M** is the diagonal mass matrix, **B** describes the acting of the moments between the components on the components, **C** describes the constraints between the mechanical parts and **D** is the relation between the moments. **a** represents accelerations, **m** describes moments in the system and **F** covers the moments calculated in the components which act on the mechanic system.

1.2 Electrical System

In hybrid electric vehicles, the electric part of the power train is strongly coupled to the mechanical system (*Fig. 2*). However, typically electrical system responds much faster compared to the mechanical system [15]. On the system level, the inductivities might be neglected [15]. Considering the latter simplification and

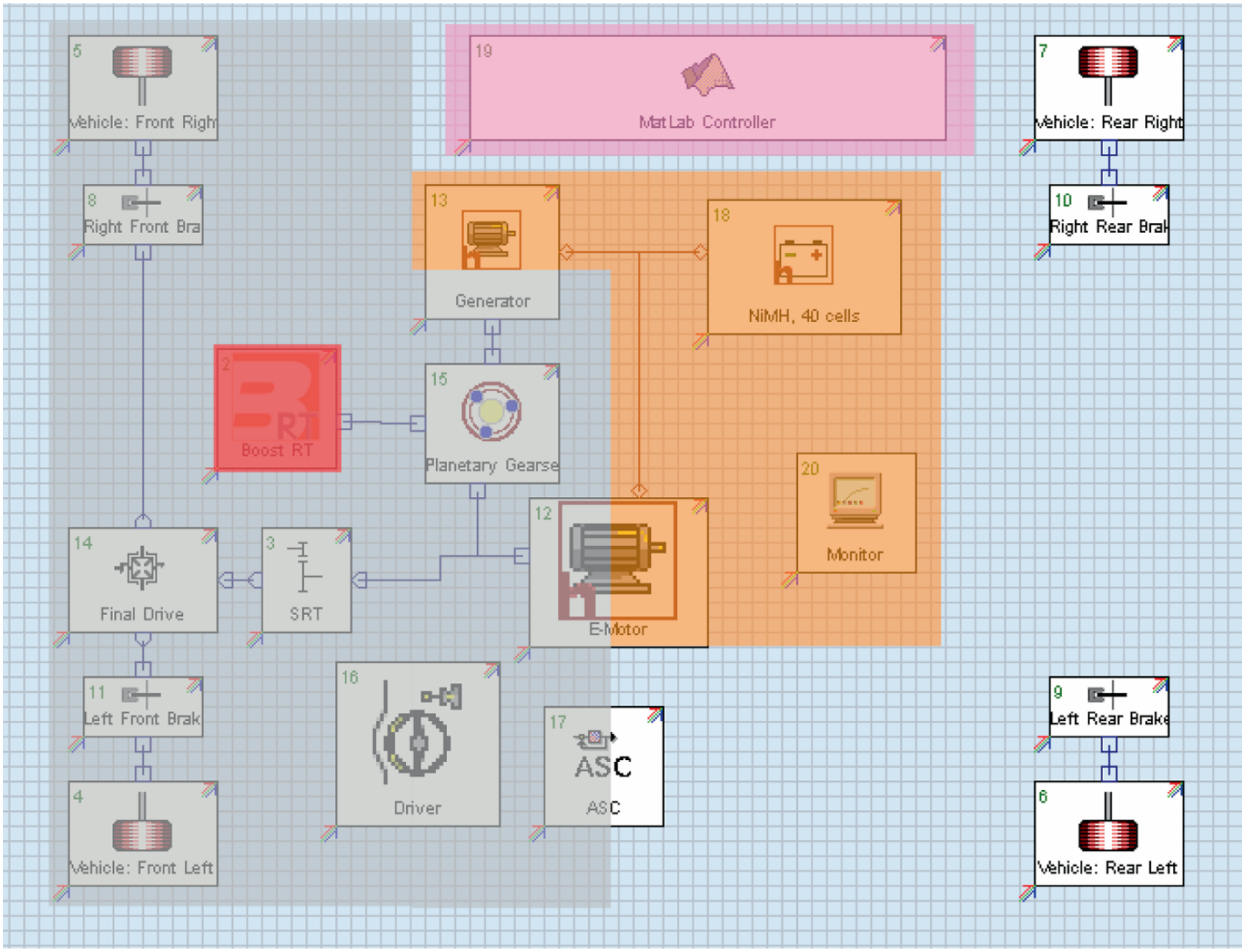

Figure 2

Topology of the hybrid electric vehicle model with indicated domains; grey – mechanical system, orange – electrical system, pink – external Matlab/Simulink controller and red – internal combustion engine shown in Figure 3.

introducing voltage as an additional variable the governing equations of the electric system might be reformulated through a single derivation to yield an index of one [15]. Due to the above characteristics an explicit integration of both, the mechanical and the electrical equations is not sufficient for a stable and accurate numerical solution [15]. In order to optimize the performance of the model it is thus beneficial to solve first for the mechanical system and then for the electrical system with assuming a frozen mechanical state [15]. This time integration step can be seen as a mixed discretization in which the mechanical variables are discretized explicitly and the electrical are discretized implicitly.

1.3 Internal Combustion Engine

Internal combustion engines (*Fig. 3*) typically feature three different characteristic time scales. The shortest time scale is associated with the in-cylinder phenomena, wave dynamics in the engine manifolds and torque oscillations at the engine shaft. A larger time scale is associated with filling and emptying the engine manifolds during transient operation of turbocharged engines or during changed throttle position. The largest time scale is associated with the thermal response of the engine.

The highest accuracy of the model would certainly be achieved if the complete engine will be modeled considering the shortest time scale. However, this will lead to

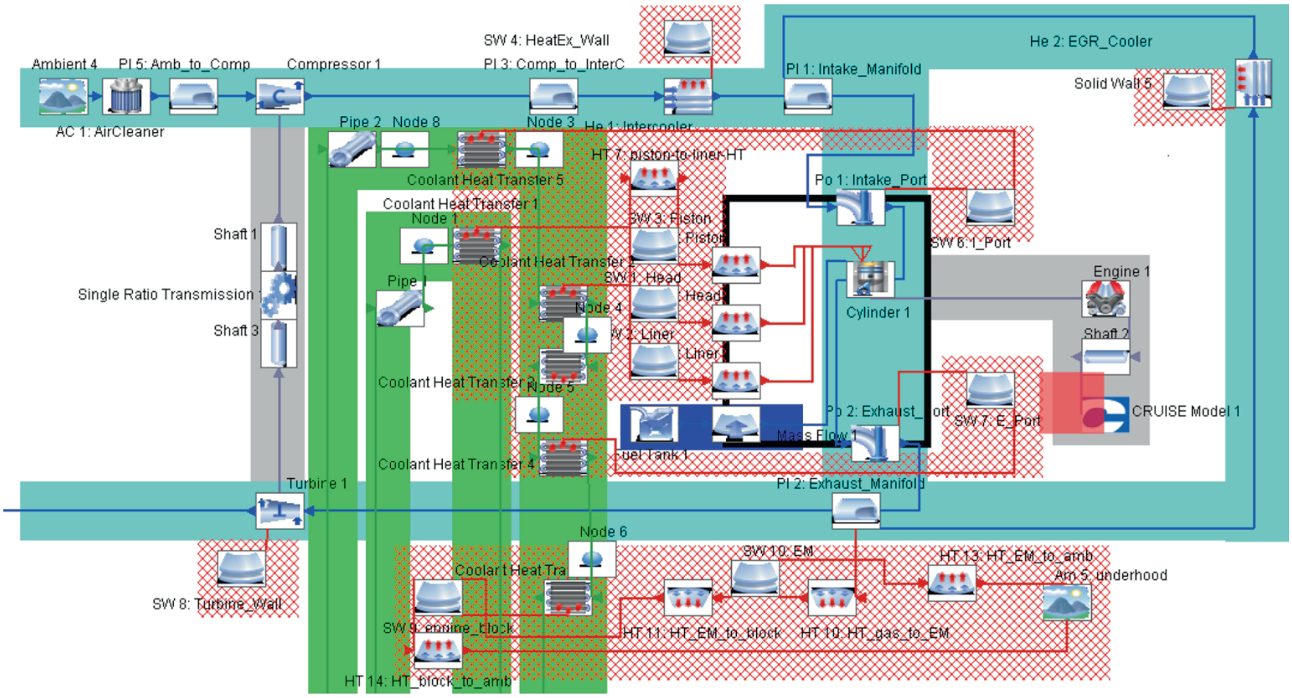

Figure 3

Topology of the engine model with indicated domains and different transfer paths; light blue – gas path of the engine, dark blue – fuelling, grey – mechanical part, red crossed – heat transfer functionality, green – liquid cooling circuits, red – vehicle model shown in Figure 2.

computational times that are characteristic for 1D cycle simulation engine models, which typically amount to approximately 100 times the physical time for complex multi-cylinder high speed engine topologies [16, 17]. Reference [18] presents a method of generating a real-time crank angle engine model from the base 1D cycle simulation engine model. The real-time model features reduced accuracy compared to the base model, whereas its real-time capability is also limited to the specific engine models.

In the present analysis, the complete hybrid vehicle model considering all domains targets to run close to or even faster than real-time. Therefore, the engine model is subjected to further optimization regarding computational speed. This is done by optimizing the code but also by reducing the level of detail of the model. The engine model therefore consists of a crank angle resolved cylinder model embedded in a mean value based gas path model (*Fig. 3*). Mean value modeling of engine manifolds does not consider wave dynamics. This is an acceptable simplification for modeling engines that do not exhibit significant enhancements of volumetric efficiency due to wave dynamics as will be shown later in the paper on an example of a passenger car turbocharged Diesel engine.

Typical integration steps of explicit solvers that ensure stable results of the mean value gas path models are in the range from 1 ms for passenger car engines up to 5 ms or even more for certain commercial vehicle engines. This is also in agreement with the data published in [19-21]. As discernable from Figure 3, the interaction between the gas path and the turbocharger dynamics as well as the EGR flow are modeled on a mechanistic basis in the mean value gas path approach. This is crucial for simulating transient engine operation [8].

To ensure a high level of predictability and accuracy during transient engine simulations it is necessary to model the cylinder with mechanistic models on a crank angle basis [8, 22]. Such an approach enables an adequate interaction of the cylinder with the intake and exhaust manifolds, since the exchange of mass, enthalpy and species masses is based on the physical models. Additionally, heat transfer and mass transfer due to fuel injection are also modeled on the crank angle basis. This is also beneficial for the adequacy of transient results, since variations in temperature of the solid structure and arbitrary injection strategies are captured. In Figure 3, the black rectangle indicates elements that exchange crank angle resolved fluxes with the cylinder. Moreover, since cylinders are calculated in a different time domain than other engine components, the components marked by the black rectangle exchange with the surrounding cycle average fluxes that are evaluated based on the crank angle resolved data.

An even bigger challenge compared to modeling engine performance is modeling engine emission. During the gas exchange phase a set of transient 0D single zone equations is solved [22], whereas during the combustion, balance equations for a generic two zone model are used [9, 23]. The two zone approach serves as a basis for evaluating a burned zone temperature, which is together with species concentrations and the pressure used to model a kinetically driven NO_x, CO and soot formation [23].

The gas property routines, which are used to evaluate the physical properties of the gaseous media, are taken from the database and depend on temperature, pressure and gas composition. The database is prepared based on the inputs of the fuel composition. In the present model, the gas composition is given by the species mass fraction of combustion products, burned fuel and fuel vapor, whereas mass fraction of air is derived from the conservation principle. These species are called active species ($\mathbf{w}_A$ in *Eq. 3*). Thereby only three species need to be transported through the system to adequately model the gas properties and thus engine performance. This significantly reduces the computational burden compared to transporting 8 or more species, which are required to appropriately cover the gas composition in the case where mass fractions of chemical elements are transported. In the model, additional passive species ($\mathbf{w}_P$ in *Eq. 3*) are introduced in the gas path model to adequately transport exhaust emissions through the engine. The application of passive species allows combining computational efficiency with the need for modeling pollutant transport in the gas path. In the analyzed case, we focus only on NO and NO_2 and thus only 5 species, *i.e.* 3 active and 2 passive, are transported through the engine, which minimizes the size of the overall equation system.

Mean value engine models are generally based on the bond-graph approach as presented in [22]. The transient variation of the state in a single storage (volume) component can be expressed by:

$$\mathbf{B} \cdot \frac{\mathrm{d}\mathbf{\Phi}}{\mathrm{d}t} = +\sum \dot{\mathbf{F}}_\mathrm{k} \tag{2}$$

where $\mathbf{B}$ is the capacity matrix, Φ is the state vector and $\dot{\mathbf{F}}_\mathrm{k}$ represents the flux vector related to the k'th attached bond (transfer component). Focusing on the description of the gas path, the state and flux vectors comprise the conservation variables for mass, energy and species. This can be expressed by:

$$\mathbf{\Phi} = [m, u, \mathbf{w}_\mathrm{A}, \mathbf{w}_\mathrm{P}]^\mathrm{T} \tag{3}$$

$$\dot{\mathbf{F}} = \left[\dot{m}, \dot{H}, \dot{\mathbf{W}}_\mathrm{A}, \dot{\mathbf{W}}_\mathrm{P}\right]^\mathbf{T} \tag{4}$$

where m is the mass and u is the specific internal energy. $\mathbf{w}_\mathrm{A}$ and $\mathbf{w}_\mathrm{P}$ represent vectors holding the mass fraction of active and passive species, respectively. Active species include combustion products, fuel burned, fuel vapor and air, where mass fraction of air is derived from the conservation principle. In analogy, the elements of the flux vector are the mass flow $\dot{m}$, the enthalpy flow $\dot{H}$ and two species flow vectors $\dot{\mathbf{W}}_\mathrm{A}$ and $\dot{\mathbf{W}}_\mathrm{P}$. More details on the gas path models and on the cylinder and emission production models are given in [8, 9, 22-24].

If the cylinders are integrated based on the crank angle, the integration time steps typically range from approximately 10 to 100 μs for automotive engines. This is at least an order of magnitude smaller that the time steps required by the mechanical network as addressed above. If the analysis does not cover vibrational modes of the drive train, as it is common in system level simulations aimed at optimizing performance and emissions of the vehicles, it is possible to exchange the data between the engine and the mechanical system with the frequency of the integration of the mechanical system or even with the frequency of engine cycles.

1.4 Catalytic Converters

Transient 1D models can be seen as a reasonable compromise to describe either single catalysts or also entire exhaust lines of lean operating engines (*Fig. 4*) with sufficient accuracy as presented in this paper and reported in [9, 24]. Transient 1D balance equations for the gas phase and the solid substrate can be applied under the common assumption that radial variations (*e.g.* flow velocity, species fractions, temperature) within a single channel and also within the entire catalyst brick are negligible. The model equations (described in detail in [9, 23, 24]) cover the effects of convection in the gas phase, heat conduction in the substrate and heat mass transfer between the two phases. Chemical reactions comprising conversion and storage reactions take place at active sites within the washcoat.

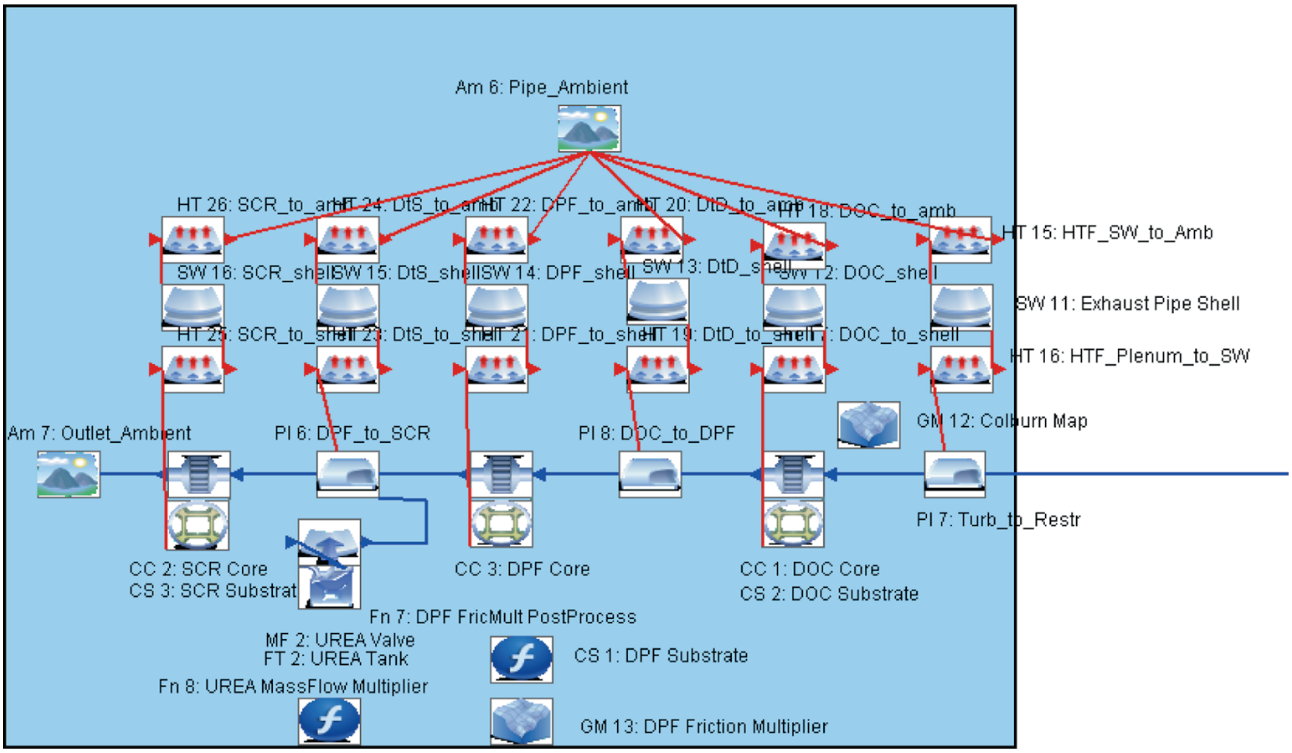

Figure 4

Topology of the exhaust gas after treatment model that is connected to the turbine of the engine as indicated in this figure and in Figure 3.

Many of the chemical reactions, which take place in catalysts, feature an exponential temperature dependency. Therefore adaptive step size solvers are mandatory to efficiently solve balance equations of catalytic converters. To optimize the overall computational time of the model, gas path and catalytic converter equations are not solved in a fully coupled system. Instead, an independent time domain of the catalytic solver allows depending on the problem, either smaller or even bigger integration time steps compared to the gas path solver. The dynamic interaction of the gas path and chemical reaction time scales thus optimizes the performance of the overall model.

1.5 Heat Transfer

The heat transfer in the vehicle power train can generally be categorized in heat transfer between components of a particular domain, heat transfer between particular domains and the cooling circuit domain and heat transfer between the domains and the surrounding as shown in Figures 3 and 4.

Heat is always transferred *via* the solid structure (*Fig. 1*). The time scale related to the thermal inertia of the solid structure is generally much larger compared to the integration time steps of the coupled mechanical/electrical solver, or of the catalytic converters solver, or of the cylinder and of the gas path solver. Therefore, the stability of governing equations of the solid structure does not represent a limitation in terms of the overall stability of the model. Elements that belong to solid structure thus provide a good basis for cross-domain coupling of domains with different time steps.

On a system level, it is common to model water and oil circuits assuming incompressible fluids. These circuits might in a single or multiple circuit topologies connect different domains, *e.g.* engine cooling and lubrication, cooling of electric components and cooling of oil in the gearbox or clutch. Considering the characteristics of water and oil cooling circuits in the automotive applications it can be concluded that they feature two characteristic time scales. The shorter one is associated with establishing the mass flow pattern, whereas the longer one is characteristic to the thermal response of the cooling circuits. Therefore and due to the fact that for incompressible flows the energy equation is not directly coupled to the continuity and momentum equation it is common to solve them decoupled, where flow equations might be solved as quasi-steady or transiently with small time steps and energy equation is solved transiently with larger time steps. Moreover, due to the fact that the characteristic time of the solid structure is also relatively large, it is beneficial to apply adaptive step size solver when solving the energy equations to reduce CPU load during steady-state operation or during slow transients. These approaches significantly contribute to optimizing computational speed of the overall model.

1.6 Control Units

The overall behavior of the vehicle is determined by the control units acting on different domains. There are two kinds of control units in the system: continuous controls and discrete controls. Continuous controls can either directly depend on input values or they can be described by a differential equation. Besides continuous states, there are also discrete variables describing the state of the vehicle, *e.g.* gear or slip-stick condition. Changes in the discrete variables cause a state event and a change in the system matrix given in Equation (1). Besides controllers that are already available in the software it is additionally possible to dynamically link controllers developed in the Matlab/Simulink.

1.7 Coupled Overall System

The model equations discussed above can be summarized to a global set of algebraic, ordinary and partial differential equations. The latter are discretized in space domain, following methods of lines to reduce all partial to Ordinary Differential Equations (ODE). In addition, second order ODE of the mechanical system are transformed into a set of first order ODE of a doubled size. This is given by:

$$\begin{aligned} \mathbf{M} \cdot \frac{d\omega}{dt} &= \tau(\omega, \varphi) \\ \frac{d\varphi}{dt} &= \omega \end{aligned} \tag{5}$$

where the system inertias represented by the mass matrix $\mathbf{M}$ times the rotational acceleration equal to all momentums. The mechanical system typically features additional linear constraints which can be substituted into the system. This framework is in the context of the presented study used for the electrical circuits.

All different states can be merged into a common state vector of unknowns x. Its time derivate multiplied with the system matrix $\mathbf{S}$ equals a right-hand-side function that depends on x and time t. This coupled system of ODE, as it is combined with algebraic constrain functions $g(x)$, leads to an overall semi-implicit Differential Algebraic Equation (DAE) system:

$$\begin{aligned} \mathbf{S} \cdot \frac{dx}{dt} &= f(x, t) \\ 0 &= g(x) \end{aligned} \tag{6}$$

where the system matrix $\mathbf{S}$ may additionally depend on the state x. The integration of the resulting DAE system in time domain is performed by tailored solver techniques suited to account for characteristic time scales of individual domains, which represent submatrices in the overall system matrix. These submatrices are integrated with time steps that correspond to characteristic time scales of the phenomena in the domains as analyzed in this section. Special emphasis is taken to preserve flux conservation while coupling different domains. This approach allows for significant improvements in the trade-off between the computational speed and accuracy as well as predictability of the model compared to the system level models where the shortest time scale dictates the integration step of the overall system.

The capability of the overall vehicle and power train model to adequately simulate transient vehicle operation was presented in [8], where chassis-dynamometer measurements were compared to the simulated results of the conventional internal combustion engine powered vehicle equipped with a 6-speed manual transmission.

2 VEHICLE MODELS

The simulations of the hybrid electric vehicle are based on the 2004 *Toyota* Prius model (*Fig. 2*). The model uses realistic data of the vehicle, tires, mechanical driveline components and electric components. For the purpose of the presented analysis the original gasoline engine was replaced by a turbocharged Diesel engine. It was assumed that the new engine is compatible with the vehicle body.

Results of the hybrid electric vehicle were compared against the results of the conventional vehicle powered by the same engine that is once operated with and once without start-stop strategy. The conventional vehicle is equipped with a 6-speed manual transmission. To enable a valid comparison between the hybrid and the conventional vehicle, a vehicle model featuring the same geometric characteristics and tires was used for simulating the conventional vehicle. However, the mass of the conventional vehicle is 140 kg lower compared to the mass of the hybrid vehicle to account for the mass of the electric components.

The aim of the presented analysis was not in using sophisticated calibration procedures to extensively parameterize the model in order to very precisely reflect performance and emissions of vehicles, whereas in addition a very sophisticated control unit models would be required to achieve this target. The aim was rather to use simple constant factors in specific semi-empiric models and to build basic control models with the goal to demonstrate a relatively high predictability and accuracy of the model along with its capability to model cross-domain interactions. This is of particular importance in early development stages, where extensive calibration cannot be performed due to lack of experimental data. Therefore it is worth noting that accuracy of all results might be further enhanced by applying more sophisticated calibration procedures and higher fidelity control models.

3 ENGINE MODEL

A 1.4 L high speed direct injection turbocharged Diesel engine with EGR was used in the simulations (*Fig. 3*). The validation of the engine model is presented in [8, 9] therefore only parameters that are meaningful for the presented analysis are shown here. Figure 5a,b shows very good agreement of the pressure traces in the gas exchange and in the high pressure phase. Good agreement in pressure traces and good agreement between measured and simulated volumetric efficiency (*Fig. 6d*) confirm that mean value gas path model is applicable for simulating engines that do not exhibit significant enhancements of volumetric efficiency due to wave dynamics. Figure 5c shows average in-cylinder temperature and temperatures in the burned and in the unburned zone. Establishing heterogeneous temperature and species concentration field is thus a prerequisite to model kinetically controlled emission formation. This is shown in Figure 5d, where a first small increase in NO_x mass due to combustion of the pilot injection is followed by a large increase in NO_x mass due to combustion of the main injection. Corresponding Brake Specific NO_x emission (BSNO) is presented in Figure 7a, *i.e.* 2 000 rpm full load.

Figure 6 additionally shows very good agreement between measured and simulated Brake Mean Effective Pressure (BMEP), Brake Specific Fuel Consumption (BSFC) and boost pressure. The agreement in these

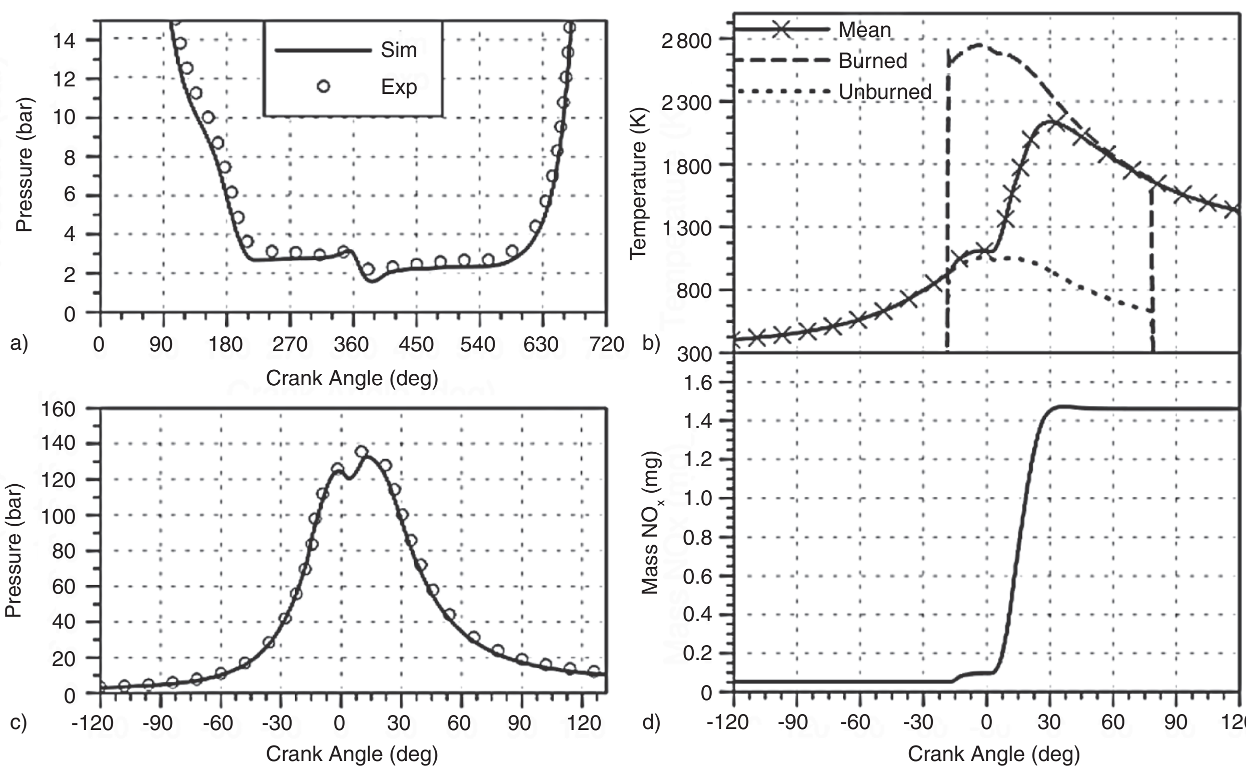

Figure 5

Comparison of measured and simulated in-cylinder pressure a) and c) using a two-zone combustion model b) at 2 000 rpm full load. Additionally, d) NO_x mass is shown.

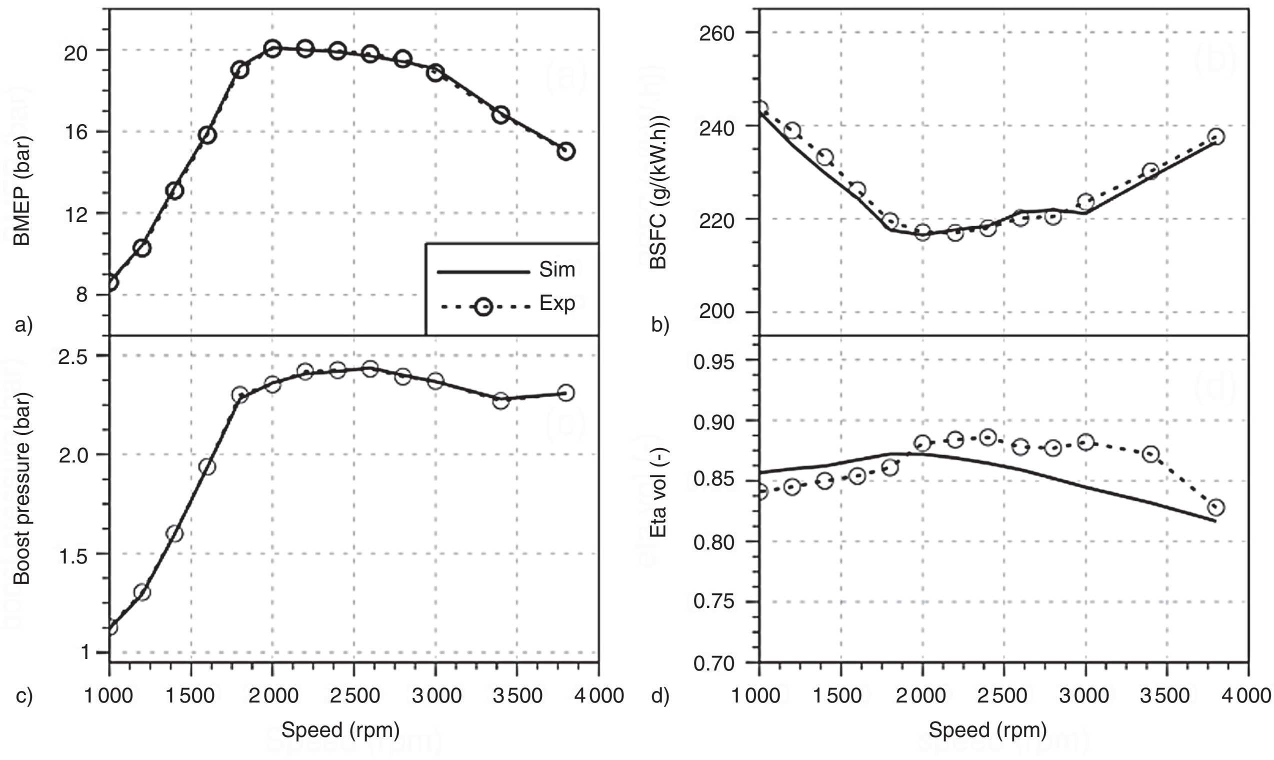

Figure 6

Comparison of measured and simulated engine full load parameters.

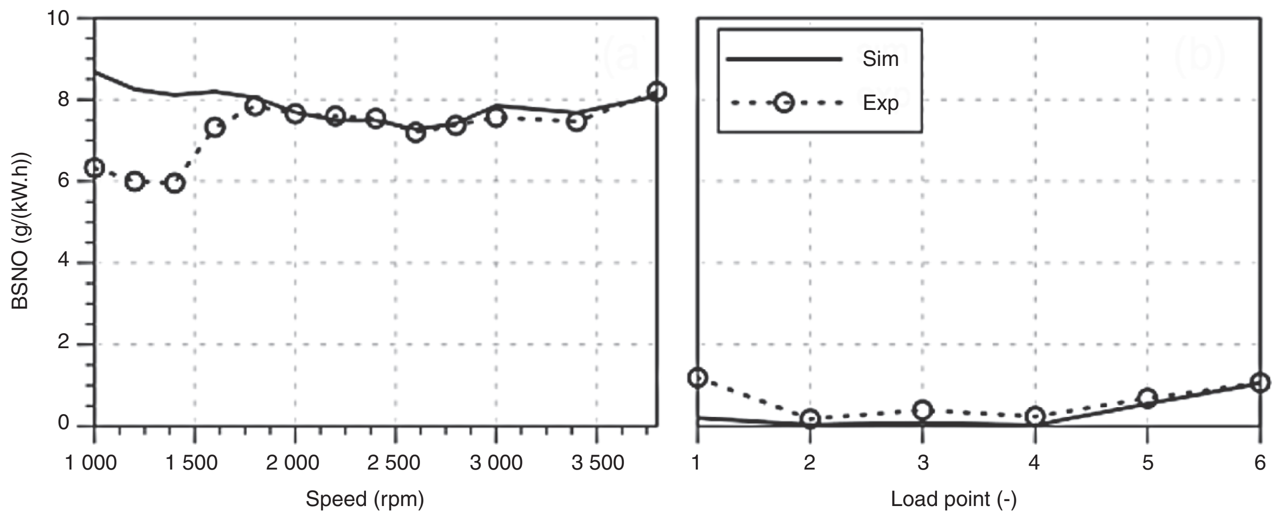

Figure 7

Comparison of measured and simulated NO_x emissions for full load operation and selected part load operation points.

parameters is even better than the agreement in volumetric efficiency. This might be attributed to the operational principles of the lean operating engines, where small deviations in fresh air mass do not significantly influence the indicated work per cycle if an adequate fuel amount is supplied and if the air-fuel ratio is sufficiently high not to significantly influence the fuel conversion efficiency. Figure 8 shows relatively good agreement between

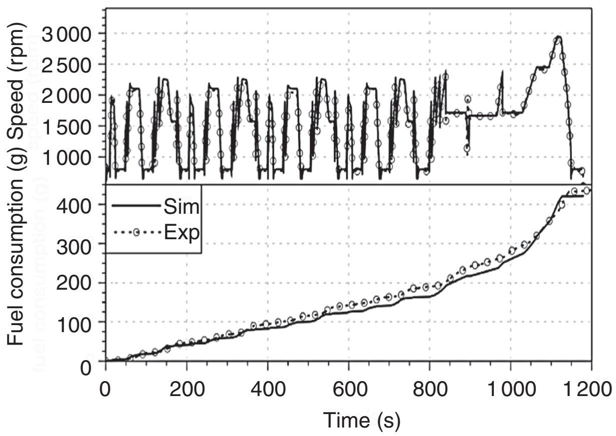

Figure 8

Comparison of measured and simulated parameters during NEDC.

measured and simulated data during transient operation of the engine. The agreement in transient results is not as good as agreement in steady-state results, which can mainly be attributed to the application of a simple engine control unit model, however quality of the transient results still presents a good basis for the presented analysis.

For the purpose of the presented analysis it is also important that the simulated emissions match reasonably well with the measured emissions. Figure 7 shows a comparison between measured and simulated NO_x emissions for full load operation and selected part load operation points [9]. It might be noted at this place that a better agreement could be achieved by performing load point dependent calibration of the model. However, to ensure adequate comparisons during the transient operation the same calibration factors were used for the whole engine operation map.

The validation of the models of catalytic converters is presented in [9, 24], whereas details on applied exhaust gas aftertreatment devices are given in [24].

4 RESULTS OF THE ECE DRIVING CYCLE

Results of the hybrid vehicle (denoted "hyb") and of the conventional vehicle operating with (denoted "conv St/St") and without (denoted "conv") start-stop strategy are presented and analyzed in this section.

The results are shown for the Engine Control Electronics (ECE) driving cycle. Due to the fact that for a cold start run catalysts do not feature any significant conversion efficiency during the first ECE cycle for all vehicles, since light off temperature is not yet reached, all vehicles were run for four consecutive ECE cycles. The results are shown only for the last ECE to preserve readability of the figures. The hybrid vehicle was operated with the neutral State of Charge (SOC) of the batteries over the last, *i.e.* forth, ECE cycle, that is analyzed in this section. Therefore fuel consumption results adequately reflect energy consumption of the vehicles.

Figure 9a indicates that all vehicles adequately follow the ECE velocity trace. Within the context of the presented forward-facing vehicle model this confirms the capability of the driver model and capability of the control unit models, which respond to the signals of the driver model, to adequately control the power flows of the power units. From Figure 9c, it is discernable that in the hybrid vehicle, the engine is turned on mainly only during vehicle acceleration and thus for a much shorter period compared to both conventional vehicles. Moreover, in the hybrid vehicle, the engine is coupled to the wheels over a planetary gear box, which enables operating the engine at much lower engine speeds. However, this results in larger values of the load signal (*Fig. 9b*) and therefore in higher values of Brake Mean Effective Pressure (BMEP) (*Fig. 9d*). Both obviously results in higher values of the peak cylinder pressure (*Fig. 9e*) – here, it might be noted that during engine off periods, the peak firing pressure is not calculated and thus the value from the last operating cycle is plotted. The operation of the engine in hybrid vehicle at lower speeds and high loads results in high effective efficiency that is most of the time above 35% (*Fig. 9f*). As a result, the hybrid vehicle consumes less fuel than both conventional vehicles (*Fig. 9g*).

At this place, it is interesting to note that the effective work (*Fig. 9h*) produced by the engine in the hybrid vehicle over the entire cycle exceeds effective works of the engines in conventional vehicles. The values in Figure 9h were obtained by integrating engine power over the entire cycle whereby only non-negative values were considered. This is justified by the fact that in the conventional vehicles the engine also frequently absorbs power during vehicle decelerations and it is thus not adequate to consider such operation when evaluating effective work produced by the engine. The effective work of the engine in the hybrid vehicle is larger mainly due to two facts. First, the hybrid vehicle features larger mass and thus more work is needed for its propulsion. Second, the transformation between mechanical and electrical energy, and transport and storage of electric energy is associated with larger losses than transport of mechanical energy in conventional vehicles. If regenerative

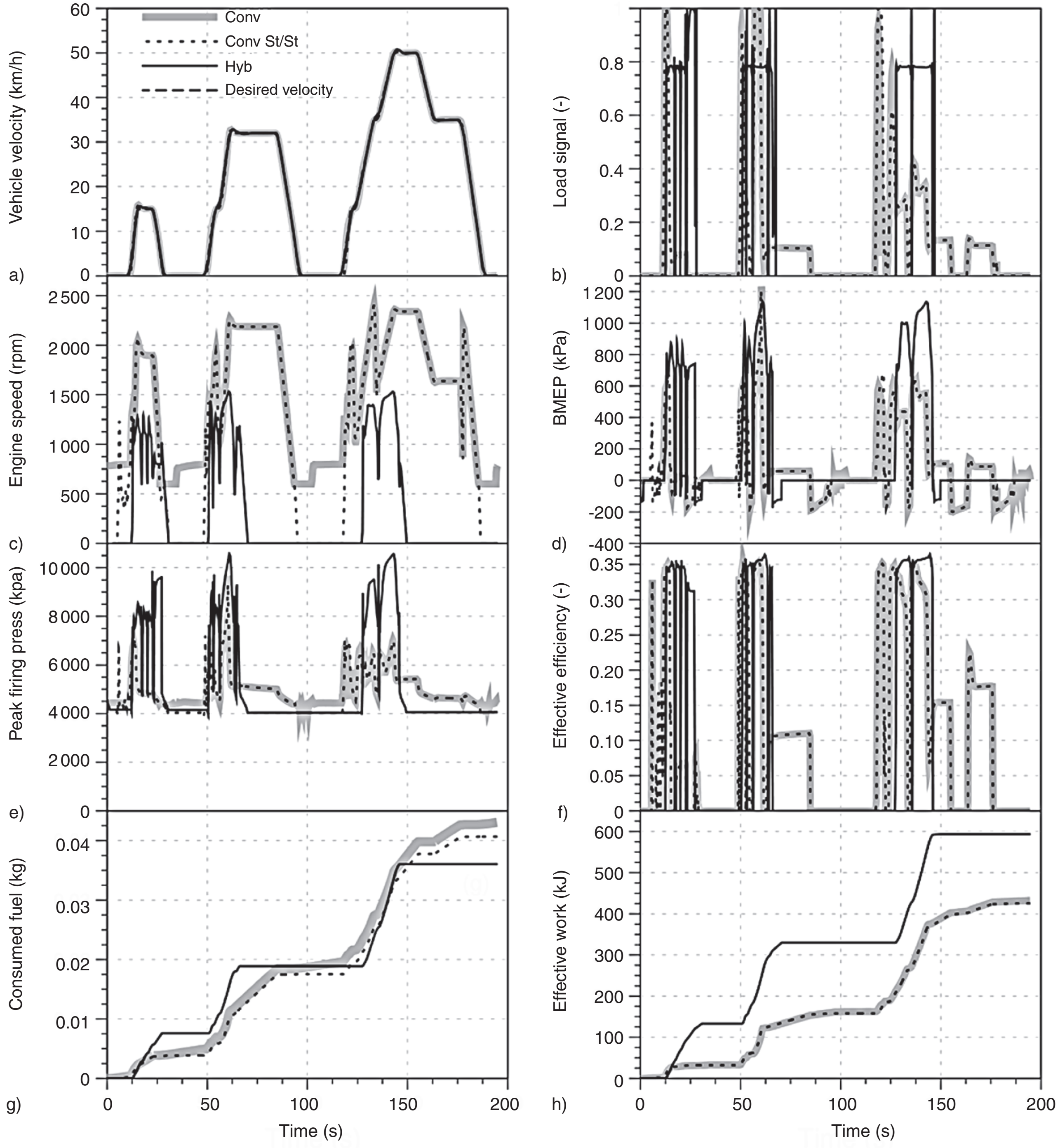

Figure 9

Comparison of engine and vehicle parameters for the ECE.

braking is not capable of compensating for all these losses, which is the case in the analyzed example, engine needs to produce more effective work to cover these losses if the hybrid vehicle is operated with neutral SOC (more details on the energy conversion phenomena in hybrid electric vehicle can be found in [25, 26]).

Figure 9 indicates that conventional vehicles are characterized by low engine loads and thus low BMEPs during

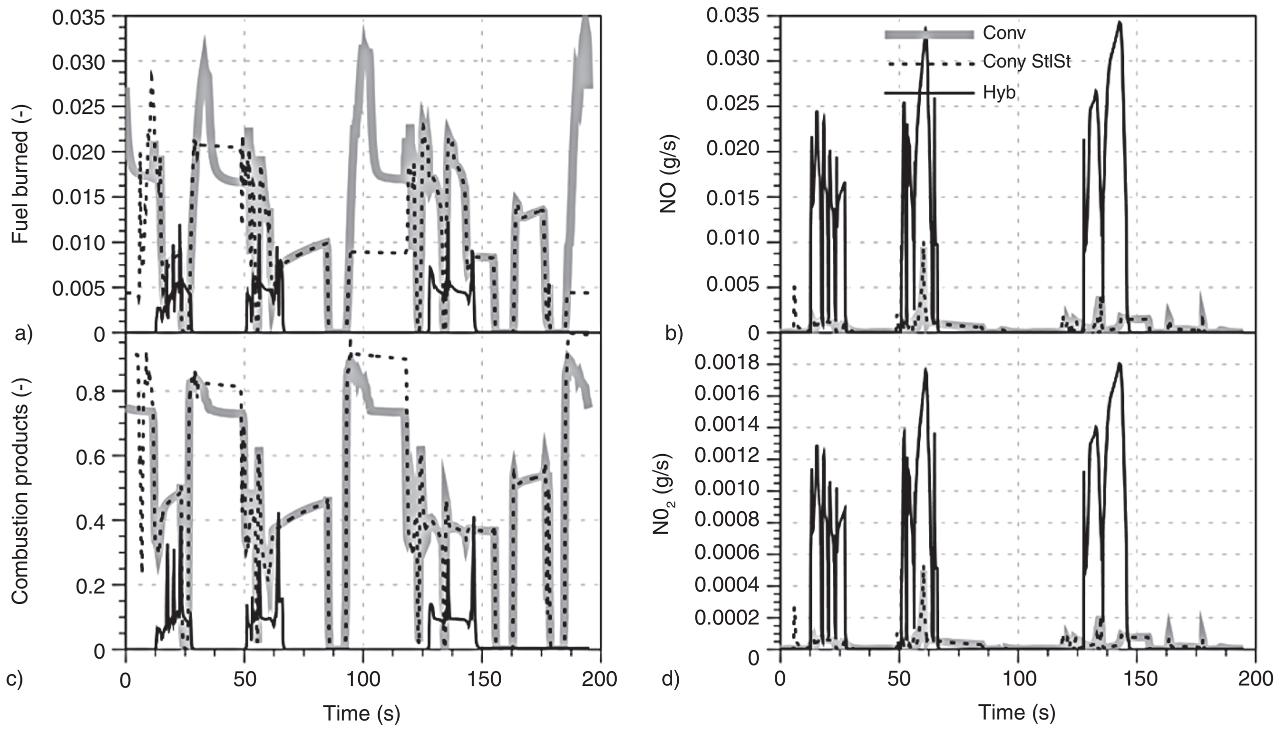

Figure 10

a) Comparison of fuel burned and c) combustion products mass fractions together with b) the engine out NO and d) NO_2 emissions.

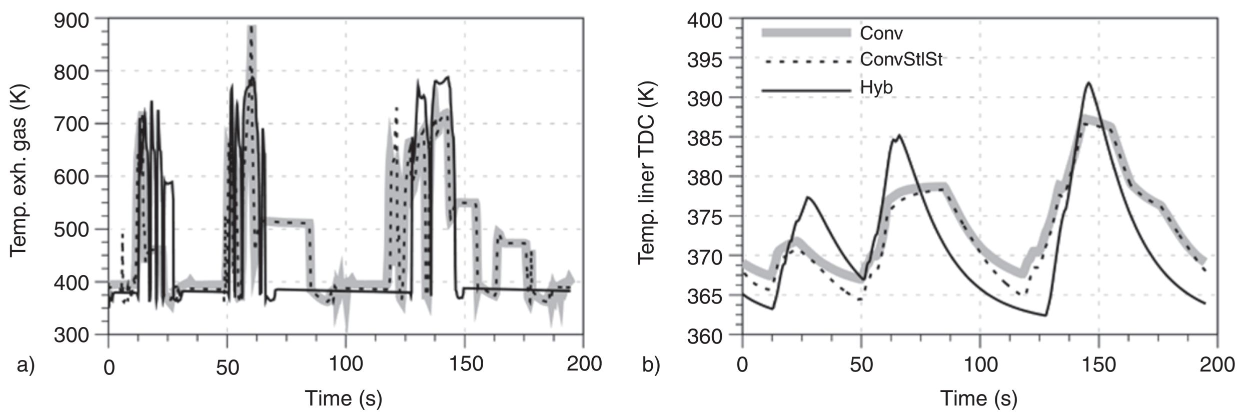

Figure 11

Comparison of: a) temperatures of the exhaust gasses in the exhaust manifold and b) temperatures of the liner at TDC.

steady-state cruising at relatively low vehicle speeds. This results in frequent operation of the engines in low effective efficiency regions (*Fig. 9f*) being the main reason for their worse fuel economy. This is slightly improved if the conventional vehicle is operated with start-stop strategy, which reduces fuel consumption during vehicle stops.

Operation of the engine at high loads is clearly favored if the fuel economy is the main objective. However, high load engine operation, which is characteristic for the engine in hybrid vehicle (*Fig. 9b*), results in very low EGR rates (*Fig. 10a,c*), since sufficient amount of oxygen should enter the cylinders to allow for complete

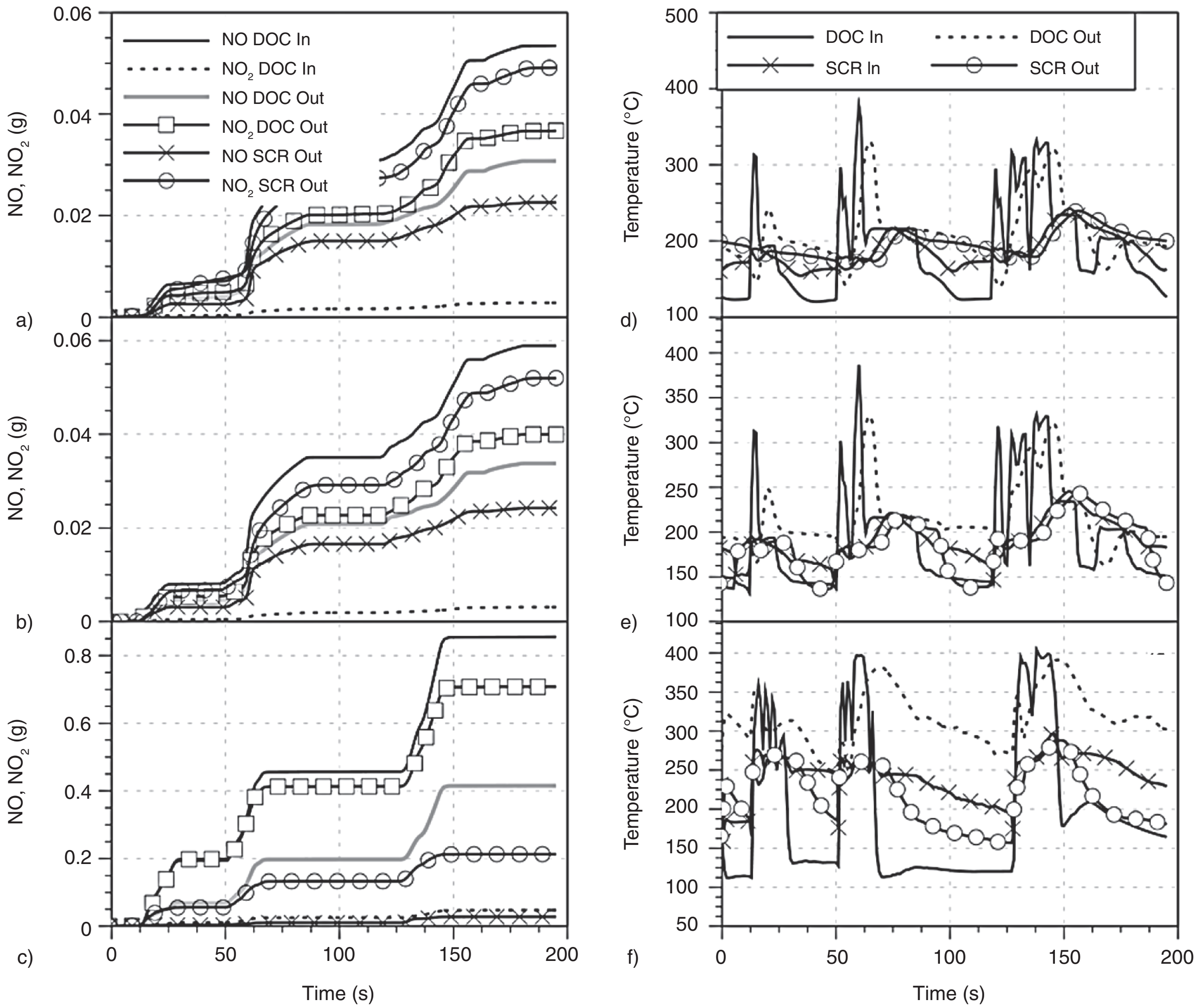

Figure 12

Comparison of: a-c) NO and NO_2 emissions and d-f) temperatures of substrates of catalytic converters at the inlet and the outlet; a) and d) conv, b) and e) conv St/St, c) and f) hyb.

combustion and sufficiently low soot emissions. Figure 10 a gives the mass fraction of the combustion products in the intake manifold (*Eq. 3*), which accounts for the contribution of the external EGR and minor potential contribution of the backflow through the intake valve. For the lean operating engines it is also necessary to consider the mass fraction of the burned fuel (*Fig. 10c*) in the intake manifold (*Eq. 3*), since it gives the information on the oxygen availability in the recirculated exhaust gasses. Due to the operation of the engine in the hybrid vehicle at high loads, *i.e.* high cyclic fuel deliveries, and with low EGR rates, the temperature of the burned zone is significantly larger than the one in the conventional vehicles leading to significantly higher engine out NO and NO_2 emissions (*Fig. 10b,d*).

Due to the operation at higher loads, the engine in the hybrid vehicle also features higher exhaust gas temperatures (*Fig. 11a*), which will positively influence the conversion rates of the catalysts. From Figure 11b, it can be seen that peak liner temperatures at the Top Dead Center (TDC) are not significantly higher for the engine in the hybrid vehicle due to longer engine off periods.

Figure 12 shows cumulative emission across the exhaust aftertreatment devices and temperature of the DOC and the SCR substrates. In Figures 12d-f, it can be seen that relatively large thermal inertia of the exhaust line (*Fig. 4*) significantly damps temperature peaks from the DOC to the SCR. This fact importantly influences the conversion efficiency of the SCR. In the case of the conventional vehicles, SCRs are not heated above the light-off temperature during operation of the engine at higher loads, *i.e.* vehicle accelerations (*Fig. 12d,e*).

As indicated in Figure 10b,d it can be seen that engine in the hybrid vehicle produces much larger engine out NO and NO_2 emissions. Engine out emissions are very similar to the DOC inlet emissions (*Fig. 12a-c*) and thus only DOC inlet emissions are shown to preserve readability of the figures. The DOC is the first device in the aftertreatment line and therefore it features sufficiently high temperature (*Fig. 12d-f*) allowing significant oxidation of NO to NO_2 for all vehicles, whereas conversion of NO to NO_2 is more pronounced for the hybrid case due to higher exhaust gas temperatures. The DOC out emissions are very similar to SCR inlet emissions and thus these results are again not shown to preserve readability of the figures.

Due to a sufficiently high SCR temperature, high NO_2 and sufficient NH_3 concentrations it can be observed that NO is very efficiently removed in the SCR of the hybrid vehicle. In the SCR, NO_2 is mainly removed in the reactions with NO and NH_3. Due to its high inlet concentration in the hybrid case, NO_2 is removed less efficiently in the SCR than the NO due to slower rate of the reaction between NO_2 and NH_3. Unlike, it can be observed that for both conventional vehicles, the temperature of the SCR is too low to enable notable NO_x reduction. Instead only partial oxidation of NO to NO_2 is observed. Comparing Figures 12a,b, it can also be observed that NO_x emissions are slightly higher if start-stop strategy is applied. This is mainly due to larger NO_x emission during engine starts.

This relatively simple example of analyzing fuel consumption and NO_x emissions over the ECE driving cycle already exposes the need for a very complex system simulation tool to perform optimization/parametric studies that are needed in the development process of the vehicle. In addition, a mechanistic basis enables modeling of the complete cause and effect chain from the in-cylinder processes to the thermal response of the catalysts and their conversion rates within a coupled multi-domain model. Moreover, mechanistic basis also enables significant benefits over data driven models when performing parametric studies and studies related to the sizing the components. One of such measures that might improve NO_x emissions of the analyzed hybrid vehicle in this specific operating regime would include reducing the size and thus also the NO to NO_2 conversion efficiency of the DOC. However in a development process of the new vehicle much more complex multi-objective optimization processes are performed, which might be effectively supported by the mechanistically based system level simulation tools.

CONCLUSION

A comprehensive mechanistic system level simulation model of a hybrid vehicle was presented in the paper. The model comprises all relevant domains, which are necessary to adequately model performance and emissions of the vehicle. It was shown in the paper that mechanistic modeling approach provides a good basis for development and optimization of hybrid and conventional power trains. This is justified by their high level of predictability and their adequacy in modeling the interaction of different domains during transient operating regime of the components. Moreover, mechanistic models are unlike map based models also able to cover highly transient operating regimes that significantly deviate from the steady-state regimes.

An adequate coupling of the domains is crucial for achieving a good ratio between accuracy, predictability and computational speed. An innovative domain decoupling approach, which is based on the characteristic time scales of different domains, is presented in the paper. This approach allows for significant improvements in the trade-off between the computational speed and accuracy as well as predictability of the model compared to the system level models where the shortest time scale dictates the integration step of the overall system. The overall real-time factor measured for an offline ECE simulation on a standard PC is in the range of 1.6 for the conventional and 1.7 for the hybrid power train, whereas real-time factors decrease below 0.9 if chemical reactions in the catalysts are not considered.

REFERENCES

1 Gao Z., Conklin J.C., Daw C.S., Chakravarthy V.K. (2010) A proposed methodology for estimating transient engine-out temperature and emissions from steady-state maps, *Int. J. Engine Res.* **11**, 2, 137-151.

2 Boland D., Berner H.J., Bargende M. (2010) Optimization of a CNG Driven SI Engine Within a Parallel Hybrid Power Train by Using EGR and an Overized Turbocharger with Active-WG Control, *SAE Technical Paper* 2010-01-0820.

3 Millo F., Badami M., Ferraro C.V., Lavarino G., Rolando L. (2010) A Comparison between Different Hybrid Powertrain Solutions for a European Mid-Size Passenger Car, *SAE Technical Paper* 2010-01-0818.

4 Isermann R., Müller N. (2001) Modeling and Adaptive Control of Combustion Engines with Fast Neural Networks. eunite, *1st International Workshop on Hybrid Methods for Adaptive Systems: Hybrid Systems* URL http://www.eunite.org.

5 Gao Z., Chakravarthy V.K., Daw C.S. (2011) Comparison of the simulated emissions and fuel efficiency of Diesel and gasoline hybrid electric vehicles, *Proc. IMechE Part D: J. Automobile Engineering* **225**, 944-959.

6 Lindenkamp N., Stöber-Schmidt C.P., Eilts P. (2009) Strategies for Reducing NO_x- and Particulate Matter Emissions in Diesel Hybrid Electric Vehicles, *SAE Technical Paper* 2009-01-1305.

7 Rakopoulos C.D., Giakoumis E.G. (2009) *Diesel Engine Transient Operation, Principles of Operation and Simulation Analysis*, Springer-Verlag, London.

8 Wurzenberger J.C., Bartsch P., Katrašnik T. (2010) Crank-Angle Resolved Real-Time Capable Engine and Vehicle Simulation – Fuel Consumption and Performance, *SAE Technical Paper* 2010-01-0748.

9 Wurzenberger J.C., Bardubitzki S., Bartsch P., Katrašnik T. (2011) Real Time Capable Pollutant Formation and Exhaust Aftertreatment Modeling-HSDI Diesel Engine Simulation, *SAE Technical Paper* 2011-01-1438.

10 Smith D., Lohse-Busch H., Irick D. (2010) A Preliminary Investigation into the Mitigation of Plug-in Hybrid Electric Vehicle Tailpipe Emissions Through Supervisory Control Methods, *SAE Technical Paper* 2010-01-1266.

11 Markel T., Brooker A., Hendricks T., Johnson V., Kelly K., Kramer B., O'Keefe M., Sprik S., Wipke K. (2002) ADVISOR: a systems analysis tool for advanced vehicle modeling, *J. Power Sources* **110**, 255–266.

12 Mierlo J., Maggetto G. (2004) Innovative iteration algorithm for a vehicle simulation program, *IEEE Trans. Vehic. Technol.* **53**, 2, 401-412.

13 Guzzella L., Sciarretta A. (2007) *Vehicle Propulsion Systems - Introduction to Modeling and Optimization*, Springer-Verlag, Berlin Heidelberg.

14 Hendricks E., Sorensen S.C. (1990) Mean Value Modeling of Spark Ignition Engines, *SAE Technical Paper* 900616.

15 Pfau R.U., Schaden T. (2011) Real-Time Simulation of Extended Vehicle Drivetrain Dynamics. Multibody Dynamics, *Comput. Meth. Appl. Sci.* **23**, 195-214.

16 Users Guide AVL BOOST VERSION 2011, Edition 07/2011.

17 Gamma Technologies GT-POWER, www.gtisoft.com.

18 Paciti G.C., Amphlett S., Miller P., Norris R., Truscott A. (2008) Real-Time Crank-Resolved Engine Simulation For Testing New Engine Management Systems, *SAE Technical Paper* 2008-01-1006.

19 Flärdh O., Gustafson M. (2003) *Mean Value Modelling of a Diesel Engine with Turbo Compound*, Sweden, Linköpings Universitet, LiTH-ISY-EX-3443-2003. Dept. of Electrical Engineering.

20 Höckerdal E. (2011) Model Error Compensation in ODE and DAE Estimators with Automotive Engine Applications, *Dissertations*, Sweden, Linköpings Universitet, No. 1366, Dept. of Electrical Engineering.

21 Mean-Value Internal Combustion Engine Model: Real-Time Execution in LabVIEWTM, *Maplesoft*, (2010) Retrieved from www.maplesoft.com on 23.07.2011.

22 Wurzenberger J.C., Heinzle R., Schuemie H.A., Katrašnik T. (2009) Crank-Angle Resolved Real-Time Engine Simulation – Integrated Simulation Tool Chain from Office to Testbed, *SAE Technical Paper* 2009-01-0589.

23 Users Guide AVL BOOST VERSION 2011: Real-Time (RT) Users Guide, Edition 07/2011.

24 Wurzenberger J.C., Bardubitzki S., Heinzle R., Katrašnik T. (2011) Physical Based Real Time System Modeling – Model and Application Workflow, *13th EAEC European Automotive Congress, EAEC 2011*, Valencia, Spain, 14-17 June, Paper A32.

25 Katrašnik T. (2009) Analytical framework for analyzing the energy conversion efficiency of different hybrid electric vehicle topologies, *Energy Convers. Manage.* **50**, 1924-1938.

26 Banjac T., Trenc F., Katrašnik T. (2009) Energy conversion efficiency of hybrid electric heavy-duty vehicles operating according to diverse drive cycles, *Energy Convers. Manage.* **50**, 2865-2878.

Final manuscript received in December 2012
Published online in April 2013